A Self-Consistent High- and Low-Frequency Scattering Model for Cirrus

Anthony J. Baran[a], Richard Cotton[a], Stephan Havemann[a], Laurent C.- Labonnote[b] and Franco Marenco[a]

[a]*Met Office, FitzRoy Road, Exeter,EX1 3 PB, United Kingdom*
[b]*Université de Lille, Laboratoire d'Optique Atmosphérique, 59655, Villeneuve d'Ascq, France*

Abstract. This paper demonstrates that an ensemble model of cirrus ice crystals that follows observed mass-dimensional power laws can predict the scattering properties of cirrus across the electromagnetic spectrum, without the need for tailor made scattering models for particular regions of the spectrum. The ensemble model predicts a mass-dimensional power law of the following form, mass $\propto D^2$ (where D is the maximum dimension of the ice crystal). This same mass-dimensional power law is applied across the spectrum to predict the particle size distribution (PSD) using a moment estimation parameterization of the PSD. The PSD parameterization predicts the original PSD, using in-situ estimates (bulk measurements) of the ice water content (IWC) and measurements of the in-cloud temperature; the measurements were obtained from a number of mid-latitude cirrus cases, which occurred over the U.K. during the winter and spring of 2010. It is demonstrated that the ensemble model predicts lidar backscatter estimates, at 0.355 μm, of the volume extinction coefficient and total solar optical depth to within current experimental uncertainties, hyperspectral brightness temperature measurements of the terrestrial region (800 cm^{-1} – 1200 cm^{-1}) to generally well within ±1 K in the window regions, and the 35 GHz radar reflectivity to within ±2 dBZ. Therefore, for simulation of satellite radiances within general circulation models, and retrieval of cirrus properties, scattering models, which are demonstrated to be physically consistent across the electromagnetic spectrum, should be preferred.

Keywords: Climate, Cloud physics, Electromagnetic spectrum, Ice crystals, Radiative transfer, Remote sensing.
PACS: 92.60.H-, 92.60.Mt,92.60.Nv,92.60.Ta,92.60.Vb

INTRODUCTION

With the advent of the 'A-train', which sample's clouds across the electromagnetic spectrum nearly simultaneously, it is important to construct scattering models of cirrus that are physically consistent across the spectrum [1]. Future satellites, such as 'EarthCARE', will carry on the concept of the A-train, but with all active and passive instruments located on the same space-based platform. However, constructing predictive scattering models of cirrus is difficult, simply because cirrus is composed of non-spherical ice crystals, which vary in size and shape, to a considerable degree [1]. Although cirrus ice crystals are complex, they do, however, approximately follow mass- and area-dimensional power laws [2]. To first order, it is these quantities that determine the radiative properties of cirrus. It is therefore, important for scattering models of cirrus to predict these basic macrophysical and microphysical properties, since the same model can then be applied across the electromagnetic spectrum to predict the high- and low-frequency properties of cirrus. In this article, it is demonstrated, using in-situ measurements of cirrus, and using the same scattering model, that it is possible to predict active and passive measurements, negating the need to apply tailor made models to particular regions of the spectrum. The condition of demonstrable physical consistency across the spectrum is a necessity in order to achieve a unified approach to climate prediction and remote sensing.

METHODOLOGY

A model of cirrus ice crystals has previously been proposed to predict the radiative properties of cirrus at solar wavelengths, called the 'ensemble model' [3]. The ensemble model consists of six elements, the first of which is the hexagonal ice column of aspect ratio (i.e., the ratio of length-to-diameter) unity, the six-branched bullet rosette, thereafter; hexagonal columns are arbitrarily attached, as a function of maximum dimension, to construct hexagonal ice aggregates, until finally a spatial ten element hexagonal ice aggregate is constructed. The single

Radiation Processes in the Atmosphere and Ocean (IRS2012)
AIP Conf. Proc. 1531, 167-170 (2013); doi: 10.1063/1.4804733

hexagonal ice column and spatial ice aggregates are distributed into six equal intervals of a PSD, representing the smallest and largest maximum dimensions of ice crystals, respectively. The PSD used to predict the bulk scattering properties is a moment estimation parameterization due to [4]. The PSD parameterization is based on 10000 in-situ measurements of PSDs, obtained in the tropics and mid-latitudes, and the PSDs were inter-arrival time filtered to remove artefacts of shattered ice crystals [4]. Other PSD parameterizations that are available in the literature use a pre-determined mass-dimensional relationship. However, Ref. [4], parameterizes the moments alone, the second moment (i.e., ice mass or IWC) is linked to any other moment via polynomial fits to the in-cloud temperature. Thus, for a given IWC, cloud temperature and assumed mass-dimensional relationship, the original PSD can be estimated.

The ensemble model predicts a mass-dimensional relationship of the following form, mass=$0.04D^2$ (SI units), where D is the maximum dimension of the ice crystal [5], this same relationship is applied across the spectrum to generate the PSDs, using [4]. The IWC and cloud temperature measurements were obtained during the CONSTRAIN field campaign, which took place during the winter and spring of 2010, and was located around the U. K. The campaign, in-situ microphysical instruments and data analysis are described in [6]. In this paper, IWC and cloud temperature measurements are utilised from four Lagrangian spiral descents, which took place in one semi-transparent cirrus case (i.e., the same cloud was sampled over a period of about six hours) and from a profile ascent, which took place in a frontal cloud. The semi-transparent cirrus case is used to test the ensemble model prediction of the volume extinction coefficient at 0.355 μm and infrared brightness temperature measurements across the terrestrial window region (800 cm^{-1} – 1200 cm^{-1}). The frontal case is used to test the ensemble model prediction of radar reflectivity at 35 GHz.

To predict the lidar-derived volume extinction coefficient at 0.355 μm, the geometric optics approximation is assumed, in which case, the volume extinction coefficient, β_{ext}, is twice the integral product of the orientation-averaged cross-section, <P>, and PSD, and is given by the following equation,

$$\beta_{ext} = 2\int < P(\bar{q}) > n(\bar{q})d\bar{q} \qquad (1)$$

where in Eq. (1) the term $n(\bar{q})$ is the PSD, integrated over a vector $\bar{q}$, which represents the ice crystal size and shape. The high-resolution infrared brightness temperature measurements are forward modelled using a PC-based radiative transfer model (Havemann-Taylor Fast Radiative Transfer Code, abbreviated to HTFRC) described in [7], and the measurement residuals are found using the method of optimal estimation. The HTFRC-retrieval scheme uses state of the atmosphere ECMWF profile data and measurements from the Airborne Research Interferometer Evaluation (ARIES) hyperspectral instrument, between the wavenumbers 800 cm^{-1} to 1200 cm^{-1}, together with a rigorous treatment of error, to obtain the most probable state vector. From the most probable state vector; the ARIES measurements are forward modelled, and differences between the measurements and forward model define the measurement residuals. The single-scattering properties of the ensemble model are calculated using the approximation described in [8], using the tabulations of the complex refractive of ice given in [9]. At the radar frequency of 35 GHz, Rayleigh scattering can be assumed, in which case, the radar backscattering cross-section is simply $\propto mass^2/\lambda^4$, where λ is the incident wavelength. The radar reflectivity, in dBZ, is then simply given by $10\log_{10}$ of the integral product of the Rayleigh equation and PSD. To forward model the radar reflectivity the ensemble model predicted mass-dimensional relationship is assumed ($m(D)=0.04D^2$).

RESULTS

The results of comparing the above-cloud lidar-derived volume extinction coefficient, at 0.355 μm, with the ensemble model predicted volume extinction coefficient, calculated from the PSDs, generated using the IWC and cloud temperature measurements obtained from the four Lagrangian spiral descents, are shown in Figure 1. The four spiral descents are shown in the same figure for reasons of brevity. The figure shows that for the first two spiral descents, the ensemble model predicts the volume extinction coefficient to within the experimental uncertainty, for all altitudes considered. For the third spiral descent, the ensemble model under estimates the lidar derivations, probably because the cloud had moved by the time the aircraft turned and returned into the cloud. For the fourth spiral descent, the ensemble model predicts the volume extinction coefficient to within the experimental uncertainty for seven of 10 altitudes considered. The total solar optical depth (i.e., integral product of the volume extinction coefficient and vertical extent of the cloud) estimated by the lidar was found to be 0.44 ± 0.11, the ensemble model predicted total optical depth is 0.41 ± 0.20. Clearly, the total optical depth predicted by the ensemble model is well within the experimental uncertainty.

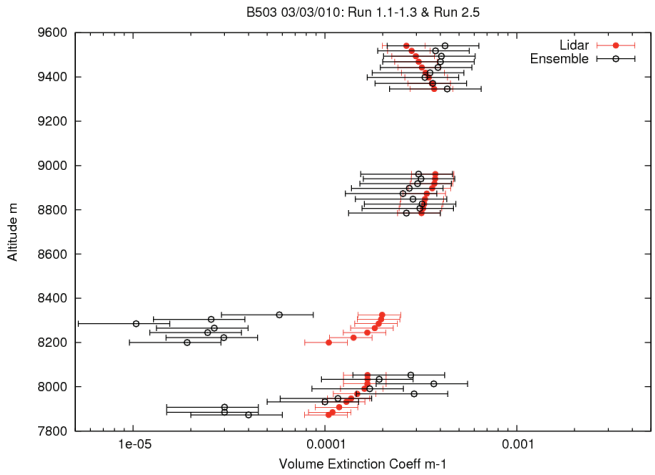

FIGURE 1. The altitude plotted as a function of volume extinction coefficient for four Lagrangian spiral descents, with the above-cloud lidar-derived volume extinction coefficients shown by the red error bars and the ensemble model predicted volume extinction coefficient shown by the error bar with open circles.

For the same above-cloud runs, shown in Figure 1, the high-resolution measurement residuals, obtained using the HTFRC-retrieval scheme, are shown in Figure 2, except for the third spiral descent.

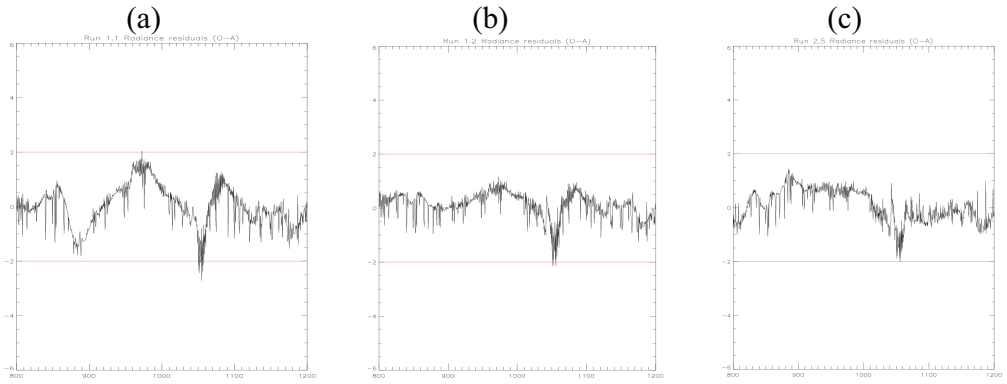

FIGURE 2. The above-cloud measurement residuals (K) plotted against wavenumber (cm^{-1}) for (a) first run above-cloud (b) second run above-cloud and (c) fourth run above-cloud. The red horizontal lines indicate ± 2 K measurement residuals.

Figure 2 shows that the measurement residuals, in the window regions, are generally within ±1 K. The largest measurement residuals occur in the wings of the Ozone absorption band, and these larger measurement residuals are most likely due to errors in the assumed Ozone profile. However, overall, the ensemble model bias is just greater than about 0 K, with no systematic bias seen in the figure.

The results of using the ensemble for forward modelling the Chilbolton 35 GHz radar reflectivity are shown in Figure 3. The figure shows that, in general, the uncertainty in the ensemble model predictions, at the beginning and middle of the profile ascent, are generally within the measured radar reflectivity uncertainty of ±2 dBZ, the model uncertainty has been derived from the IWC measurement uncertainty. The peak of the radar reflectivity at an altitude of about 4500 m is well predicted by the ensemble model. However, between the altitudes of about 6500 m and 7000 m, the ensemble model under predicts the radar reflectivity measurements. This under prediction is most likely due to the cloud horizontally advecting, by the time the aircraft reached those altitudes.

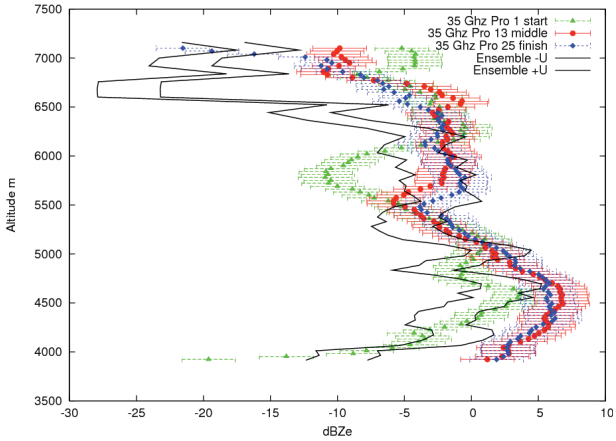

FIGURE 3. The altitude plotted as a function of radar reflectivity at 35 GHz, the uncertainty in the ensemble model predicted radar reflectivity is shown as the full lines, and the measured radar reflectivity at the beginning of the aircraft profile ascent is represented by the green error bars, middle, red error bars, and end, by the blue error bars, respectively.

CONCLUSIONS

In this paper, a high- and low-frequency scattering model for cirrus has been presented. The model consists of an ensemble of ice crystals that follows observed mass-dimensional relationships. When the ensemble model is coupled to a parameterized PSD, using the same mass-dimensional relationship across the electromagnetic spectrum, the model has predictive quality in forward modelling active and passive measurements from across the spectrum. Using aircraft-based measurements the coupled cloud physics-scattering model has been demonstrated to predict the lidar-derived, at 0.355 μm, volume extinction coefficient, and total solar optical depth, to within experimental uncertainty. The model also predicts high-resolution infrared brightness temperature measurements, between the wavenumbers 800 cm^{-1} to 1200 cm^{-1}, to within ± 1 K in the "window" regions as well as 35 GHz radar reflectivity to within ± 2 dBZ. The paper demonstrates that scattering models, which follow observed power laws, coupled to physically based PSD parameterizations, are applicable across the spectrum, without the need for tailor made models that apply only to particular regions of the spectrum. Coupled scattering models should be applied to climate models and remote sensing of cirrus properties, in order to achieve a more unified approach to the inverse problem and to the theoretical problem of climate prediction.

ACKNOWLEDGMENTS

Airborne data was obtained using the BAe-146-301 Atmospheric Research Aircraft (ARA) flown by Directflight Ltd. and managed by the Facility for Airborne Atmospheric Measurements (FAAM), which is a joint entity of the Natural Environment Research Council (NERC) and the Met Office. The Chilbolton 35 GHz radar data was provided by staff at the Science and Technologies Facilities Council.

REFERENCES

1. A. J. Baran, *J. Atmos. Res*. **112**, 45-69 (2012).
2. C. G. Schmitt and A. J. Heymsfield, *J. Atmos. Sci.* **67**, 1605-1616 (2010).
3. A. J. Baran and L.-C. Labonnote, *Q. J. R. Meteor. Soc.* **133**, 1899-18912 (2007).
4. P. R. Field, A. J. Heymsfield and A. Bansemer, *J. Atmos. Sci*. **64**, 4346-4365 (2007).
5. A. J. Baran, A. Bodas-Salcedo, R. Cotton and C. Lee, *Q. J. R. Meteor. Soc*. **137**, 1547-1560 (2011).
6. R. Cotton, P. R. Field, Z. Ulanowski and E. Hirst, in press *Q. J. R. Meteor. Soc. (2012).*
7. S. Havemann, *Proc. SPIE Int. Soc. Opt. Eng.* **6405**, doi:10.1117/12.693995 (2006).
8. A. J. Baran, *Appl. Opt*. **42**, 2811-2818 (2003).
9. S. G. Warren and R. E. Brandt, *J. Geophys. Res*. **113**, D14220, doi:10.1029/2007JD009744 (2008).